Eur. J. Mech. B/Fluids

THREE-DIMENSIONAL SURFACE WAVES PROPAGATING OVER LONG INTERNAL WAVES

J.R. Stocker and D.H. Peregrine* [1]

[1]: *School of Mathematics, University of Bristol, University Walk, Bristol BS8 1TW, England*

(Received 15 September 1998, revised and accepted 12 December 1998)

Abstract – A non-uniform current, such as may be generated by long internal waves, interacts with short surface waves and causes patterns on the sea surface that are of interest. In particular, regions of steep breaking waves may be relevant to specular radar scattering.

A simple approach to modelling this problem is to take a set of short, surface waves of uniform wavenumber on the sea surface, as may be caused by a gust of wind. The direction of propagation of the surface waves is firstly taken to be the same as that of the current, and surface tension and viscous effects are neglected. We have a number of methods of solution at our disposal: linear (one-dimensional) ray theory is simple to apply to the problem, a nonlinear Schrödinger equation for the modulated wave amplitude, modified to include to effect of the current, can be used and solutions can be found using a fully nonlinear irrotational flow solver. Comparisons between the 'exact' nonlinear calculations for two dimensions (which are too complicated/ computationally intensive to be extended to three dimensions) compare well with the two approximate methods of solution, both of which can be extended, within their limitations, to model the full three-dimensional problem; here we present three-dimensional results from the linear ray theory.

By choosing such a simple (although we consider physically realistic) initial state of uniform wavenumber short waves and assuming a sinusoidal surface current, we can reduce the two-dimensional problem to dependence on three non-dimensional parameters.

In three-dimensions, we consider an initial condition with a uniform wavetrain at an angle α say, to the propagating current, thus introducing a fourth parameter into the problem. Extension of the linear ray theory from one space to two space dimensions is numerically quite simple since we maintain uniformity in the direction perpendicular to the current, and the only difficulty lies with the presentation of results, due to the large number of variables now present in the problem such as initial wavenumber, angle of propagation, position in (x, y, t) space etc. In this paper we present just one solution in detail where waves are strongly refracted and form two distinct foci in space-time. There is a collimation of the short waves with the direction of the propagating current. © Elsevier, Paris

1. Introduction

Non-uniform currents interact with short surface waves and the resultant patterns on the sea surface are of interest. In particular, regions of steep breaking waves may be relevant to specular radar scattering. The scale of these currents may be very large, such as those generated by tidal flow over the edge of the continental shelf, or else relatively small, such as flow into an estuarine channel.

Two substantial review papers have been published in this research field. Firstly, Peregrine [1] was concerned with both large and small scale currents, currents varying with depth, and turbulence. Jonsson [2] took more of an engineer's - as opposed to an applied mathematician's - view of wave-current interactions, discussing both ocean and coastal areas.

* Author to whom correspondence should be addressed, e-mail: d.h.peregrine@bris.ac.uk, tel:+44(0)117 928 7971, fax:+44(0)117 928 7999.

This paper concerns itself with the particular interaction between short surface waves and a surface current generated by long internal waves. The problem considered is similar to that discussed by Gargett and Hughes [3]. They chose a constant frequency initial condition for the short surface waves, and considered the effect of the current in time. We take a constant wavenumber initial condition which, due to the Doppler shift caused by the current, involves a whole range of frequencies initially and in time, leads to focussing of the waves by the current. We consider this to be a more generic form of initial condition.

The two-dimensional problem is discussed in Donato, Peregrine and Stocker [4] (hereafter referred to as DPS). A simple, linear, two-layer model was used for the internal wave which gives a sinusoidal surface current. The surface current is incorporated into a fully nonlinear irrotational flow solver (first used by Dold and Peregrine, [5]) to obtain surface profiles which show the effect in time of the current on the short waves. The effect of variation of current magnitude, length of the initial short surface waves and initial steepness are discussed. Ray theory is used for the linear problem to discuss focussing of the short waves, and surface profiles were generated for comparison with results from the fully nonlinear irrotational flow solver. Ray theory (which is presented in this context by Crapper, [6]) is based on the assumption that wave properties vary slowly in time. This leads to solutions which are valid away from those regions where neighbouring rays cross, that is, at caustics and foci.

As the extension of the fully nonlinear irrotational flow solver to three dimensions is computationally impractical (at present), we use linear ray theory to obtain three-dimensional solutions. To set the scene, we first briefly present solutions for two dimensions; that is, we take the direction of the surface waves to be that of the (uni-directional) surface current. Then, we consider the three-dimensional situation where the short waves are initially at an angle to the propagating current. As there are many parameters now present in this problem, in the present paper, we restrict ourselves to the discussion of a case where the waves are strongly refracted i.e. they focus, and they initially propagate, relative to the current, at an angle of $\pi/6$ to the current. This particular case is of interest in that two foci form, whereas at small angles to the current only one focus forms, as in the two-dimensional problem.

Another method which can be extended to model the three dimensional problem is to consider a modulated, weakly nonlinear wavetrain. Its amplitude and phase are described by a nonlinear Schrödinger equation modified to include to a large-scale weak surface current. Solutions generated using this nonlinear equation are valid when the surface waves form part of a single, slowly varying wave train and are therefore only useful prior to focussing or wave breaking.

Note that our model does not allow any current modification by the surface waves. That is, we allow the surface current to remain sinusoidal for all time. Some theoretical approaches do include the wave-current coupling, for example Rizk & Ko [7], and it would be possible here, but this is not the focus of our attention.

In section 2 we discuss the model used, and reduce the problem to a four-parameter problem. A discussion of the ray theory method used is briefly given in section 3. Justification for the use of ray theory is given in section 4 by comparison with the fully nonlinear potential solver in two dimensions. Section 5 shows results using the three-dimensional ray theory when the current and initial short surface waves are at an angle of $\pi/6$ to each other. Our conclusions are given in section 6.

2. Model

The model used is the same as that described in DPS so this account is brief. The fluid is taken to be inviscid and incompressible and the short surface waves considered are taken to be long enough such that surface tension effects can be neglected but short enough to be locally independent of any density stratification. A simple, linear, two-layer model for the internal wave is used. This results in a sinusoidal form for the internal wave, and the corresponding surface current. We take an $(\hat{x}_1, x_2, y, t)$ coordinate system, where y is measured vertically upwards, $\hat{x}_1$ and x_2 are on the 'sea' surface and t is time. The frequency and wavenumber of the internal wave are taken to be Ω and $(K, 0)$ respectively and are related by

$$\Omega^2 = \frac{gK(\rho_2 - \rho_1)}{\rho_1 + \rho_2 \coth K h_1}, \tag{1}$$

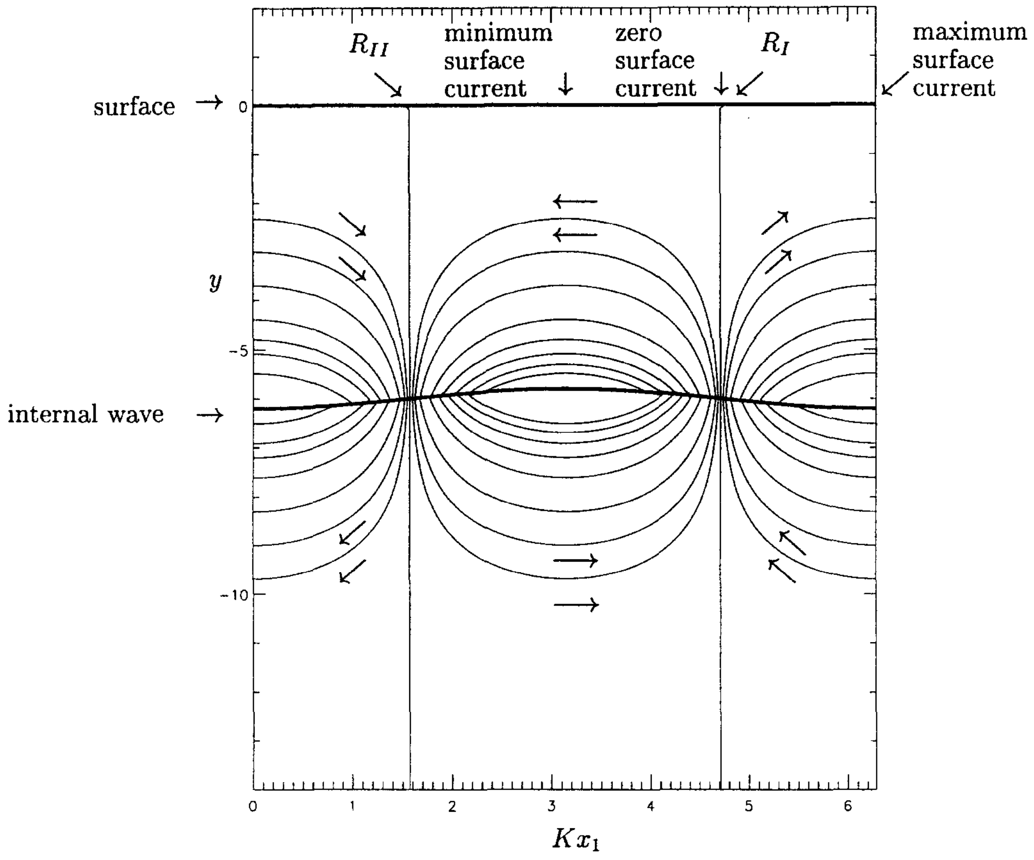

FIGURE 1. Streamlines in the two-layer internal-wave model.

where g is the acceleration due to gravity and ρ_1 and ρ_2 are the densities of the upper and lower layers respectively. The uni-directional current is aligned along the $\hat{x}_1$ axis with surface current, $\underline{U}= (U_1, 0)$ where $U_1 = U_c \cos(K\hat{x}_1 - \Omega t)$ and U_c being the maximum magnitude of the current.

Although here we have considered a two-layer model, our analysis and results are also valid for any plausible density stratification where the uppermost streamline is sinusoidal. In addition, we assume that the surface waves themselves have no effect on the stratification, as they are short enough such that the upper layer can be considered deep. However, in time, the large scale modulation induced by a non-uniform wavetrain may change the form of the internal wave. It is possible to add in a linear perturbation to model this change in waveform, but for this unsteady problem of initially constant wavenumber, we do not expect to see any large effects due to this modulation, and so have not included such effects here.

For presenting some of the results, we move into a frame of reference (x_1, x_2, t) moving with the phase speed V of the surface current, where $x_1 = \hat{x}_1 - Vt$. In this frame of reference the current becomes steady: $U_1(x_1, x_2) = U_c \cos(Kx_1) - V$ and we give streamlines of the flow in a vertical section in figure 1. Also, note that length and time are non-dimensionalised with $1/K$ and $\sqrt{gK}$ respectively.

The initial condition considered on the 'sea' surface is a uniform wavetrain of wavenumber $\underline{k_0}$ and amplitude a_0 at time $t = 0$ and an angle α_0 to the propagating current. As the short, surface waves are propagating over long internal waves, $|\underline{k_0}| = k_0$ is taken to be very much greater than K. The uni-directional nature of the propagating current together with this simple initial condition combine to imply uniformity in the x_2-direction and hence the wavenumber component in the x_2-direction remains constant, $k_2 = k_0 \sin\alpha_0$.

By choosing such a simple (although we consider it to be physically sensible, for example after a gust of wind) initial state and assuming a sinusoidal surface current, we can reduce this three dimensional problem to four non-dimensional parameters: two velocity ratio parameters, θ and γ defined by

$$\theta = \frac{U_c}{V} \qquad \text{and} \qquad \gamma = \frac{c_1}{V} = \left(\frac{g}{k_0}\right)^{\frac{1}{2}} \frac{1}{V}, \tag{2}$$

where g is acceleration due to gravity, k_0 and c_1 are the initial wavelength and phase speed respectively of the short waves, V is the phase speed of the internal wave and U_c is the maximum magnitude of the surface current. The third parameter is the initial steepness of the short surface waves which is just a simple multiplier for linear theory, and the fourth is α_0, the angle between the propagating current and the initial wavenumber of the short waves. Taking $\alpha_0 = 0$ reduces the problem to a three parameter problem which models the two dimensional case.

An alternative initial condition, considered in the two-dimensional case by Gargett and Hughes [3], is the case of considering the frequency, ω, to be initially constant everywhere. This simplifies the analysis as the frequency remains constant along rays. It is a physically realistic initial condition, for example in the case of a free surface wave packet approaching a region of surface current. In this constant frequency case, for certain physical parameters, waves are trapped in a region between two caustics either side of the position of maximum current. At this point of maximum current, waves travelling with the current are propagating much faster than those against the current. That is, there is a region of both very short and very long waves superposed at the point of maximum current. This is discussed further in DPS.

In this paper we give particular attention to waves which are strongly refracted and focus in space-time. That is, we choose to show results for only one value of $(\theta, \gamma) = (0.122, 2.416)$. These values correspond to, for example, 300 short waves on an internal wave of wavelength 120 m, pycnocline depth 6 m, with density difference of the two layers 2.5 parts per thousand and a surface current of strength approximately 0.04 m/s. An investigation into how the two-dimensional wave properties vary in the (θ, γ) phase plane is given in DPS.

3. Method of solution

Ray theory assumes that at any particular point the solution locally looks like an infinite periodic plane wavetrain so that any variations in wave amplitude, a, frequency ω and wavenumber $\underline{k}$ are slow.

The short surface wave dispersion relation is:

$$(\omega - \underline{U}\cdot\underline{k})^2 = gk \tag{3}$$

where $k = |\underline{k}|$ is the wavenumber of the short waves and ω is the frequency. This is solved along with the ray equations:

$$\frac{\mathrm{d}\underline{x}}{\mathrm{d}t} = \underline{U} + c_g\hat{\underline{k}} \tag{4}$$

where c_g is the group velocity for surface waves in the absence of a current, $\hat{\underline{k}} = \underline{k}/k$, and $\mathrm{d}/\mathrm{d}t$ defines differentiation along a ray. In our case where we have moved in to a frame of reference where the current is steady, $\underline{U} = (U_c\cos(Kx_1) - V, 0)$ and $\underline{x} = (x_1, x_2)$. The frequency, ω, is then constant along each particular ray - the value being defined by the initial conditions - and values for the wavenumber, $\underline{k}$, along the rays are obtained by solution of (3) and (4). We generate surface profiles using the conservation of wave action equation to obtain wave amplitude, and a phase equation, both of which are valid along the rays. Details are omitted and the reader is once again referred to DPS. Representations of the free surface are generated from this information and results can be compared in the two-dimensional case to those from a fully nonlinear potential solver which has been adapted to include a sinusoidal surface current. Details of this latter code are given in Dold and Peregrine [5] and the alterations made to include the current are given in DPS.

4. Two-dimensional results

Figure 2 shows a space-time ray diagram for the values of $(\theta, \gamma) = (0.122, 2.416)$. Two wavelengths and over one period of the internal wave are shown. The maximum and minimum values of the surface current are indicated by lines (– – ––) and (– · – · –) respectively. Note that these results are given in the fixed frame of reference $(\hat{x}_1, t)$. The rays are seen to focus at approximately $t = 65$, and the points of ray reflection in the frame of reference moving with the phase speed of the internal wave are indicated by an asterix. Figure 3 shows the corresponding results from the fully nonlinear code, and it is clear the linear ray theory predicts the focussing and corresponding steepness of the waves well [2]. Here we have started the nonlinear calculations with 20 waves of steepness $a_0 k_0 = 0.01$. This is due to the fact that it is computationally impractical to compute hundreds of short waves - the values of U_c and V have been adjusted in the calculation to correspond to the physical situation described in section 2 with the same values of θ and γ. The fully nonlinear code calculates solutions up to 'wave breaking'; that is, until there are insufficient points in regions of high surface curvature to obtain solutions within the accuracy required. However, as the results we present in this paper are from linear ray theory, we restrict ourselves to the less steep waves which do not break. Further calculations and discussions of the steeper waves are to be found in DPS.

The profiles shown in figure 3 have been given a vertical exaggeration of 40:1, and the regions R_I and R_{II} from the streamline pattern in figure 1 are indicated. As we have chosen values of θ and γ which correspond to waves that are strongly refracted, we can see in region R_I, where the streamlines are diverging, the waves become longer and less steep. Conversely in region R_{II}, where the streamlines are converging, the waves become shorter and steeper. This intuitive simplification of how the surface current effects the short waves is useful in explaining some of the three-dimensional effects we find later.

As mentioned previously, in regions where neighbouring rays meet, ray theory breaks down as variation in wave properties is too rapid: the wave action equation predicts infinite amplitudes. We therefore present results with a cut-off steepness value, taken to be $ak = 0.40$. The results could be improved by including diffractive effects using Airy functions at caustics and the Pearcey cusp function at the focus (for example, see Marston [8] for further details). Since we have exact solutions such as in figure 3, this extension is not followed here.

Figure 4(a) compares the fully nonlinear results (full line) with the linear ray theory results (dotted line), for non-dimensional time $t = 60$. We see that the comparison is good away from the region just before the focus where the amplitude predicted by the ray theory is too large. Figure 4(b) makes the same comparison at $t = 106$, some time after the focus. Here the waves tend to be in the same place for both the linear and nonlinear results, but the waves outside the caustics in the nonlinear case are less steep than predicted by ray theory implying that nonlinear self focussing may be acting on the energy between the caustics. Figure 4(c) shows the region between the caustics in more detail. The steep group of waves close to the left hand caustic has travelled faster in the nonlinear case which is to be expected as steeper waves travel faster than small amplitude linear waves. Also, the short waves just outside the left hand caustic are not predicted by ray theory, although matching using an Airy function does predict a wave profile of this type (Peregrine, [1]).

We conclude that the linear ray theory gives good results where waves are not too steep and in regions away from rapid variations in wave properties. Therefore we have some confidence in results from three-dimensional ray theory calculations which cannot be compared to a fully nonlinear model.

[2] Note that figures 2 and 3 correspond to figures 4 and 5 in DPS.

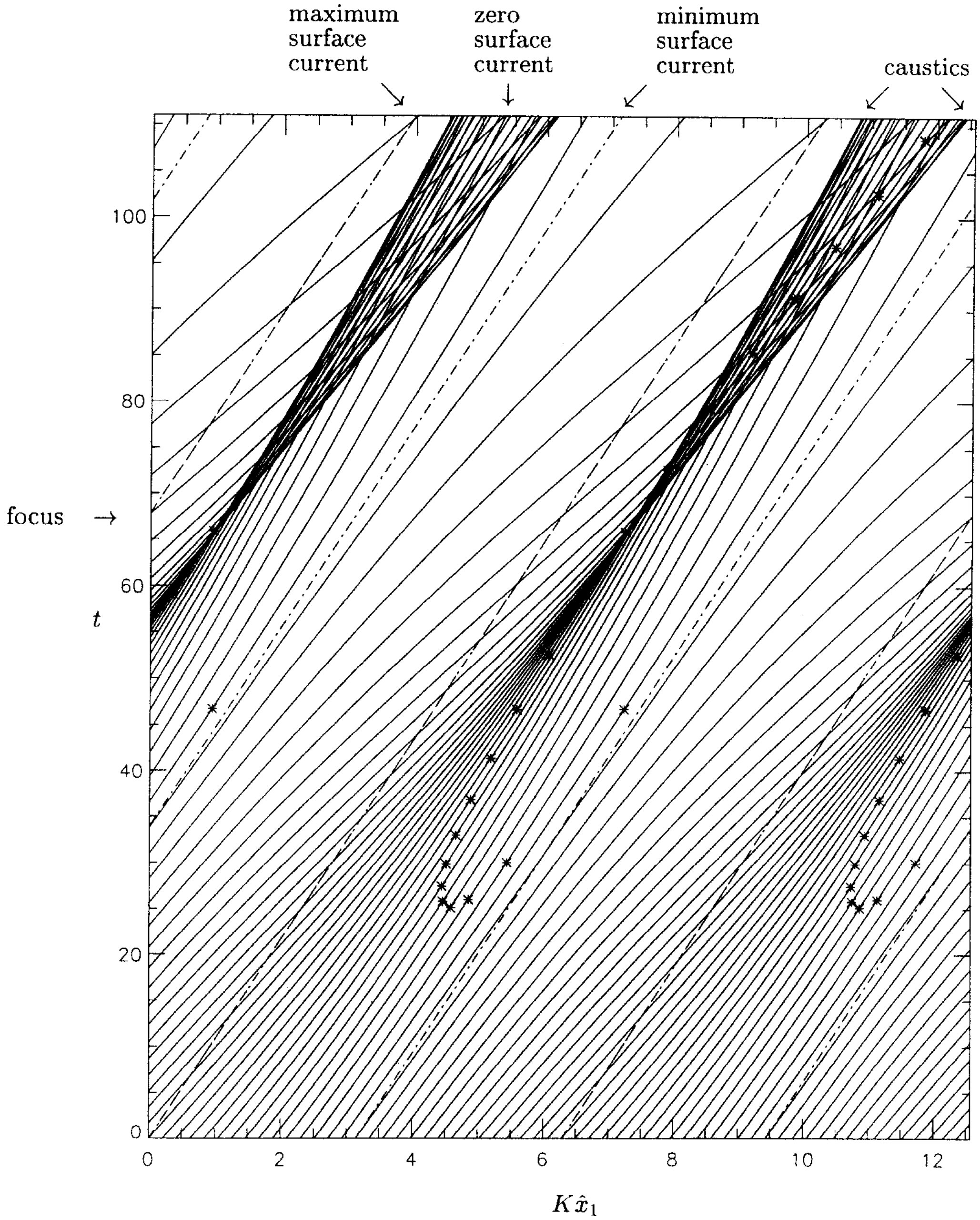

FIGURE 2. Ray diagram: the frame of reference is fixed, surface current $= U_c \cos(\hat{x} - 0.093t)$ and $(\theta, \gamma) = (0.122, 2.416)$.

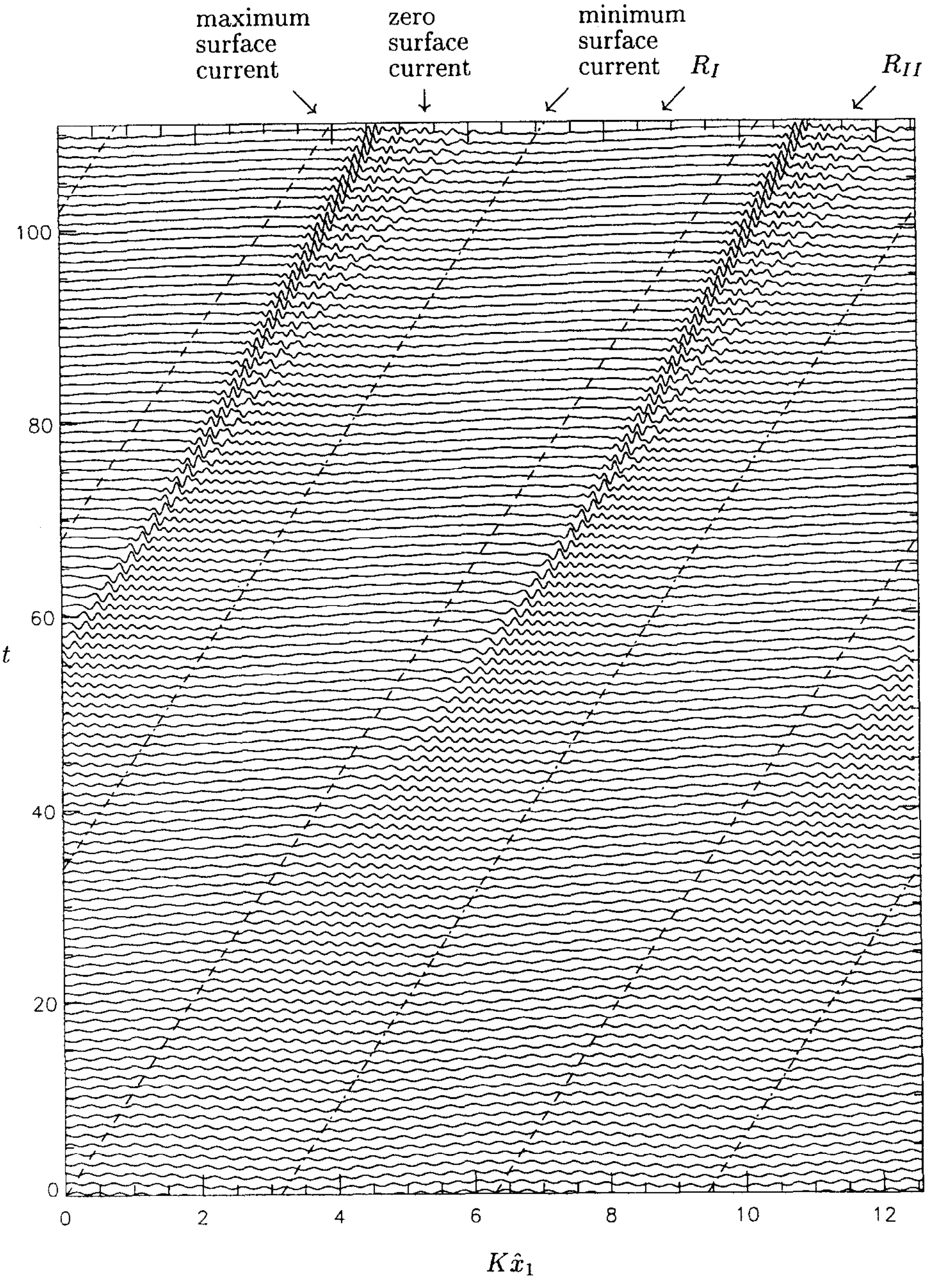

FIGURE 3. Fully nonlinear results: standard case. The frame of reference is fixed. Surface current $= U_c \cos(\hat{x} - 0.093t)$, $(\theta, \gamma) = (0.122, 2.416)$, initial steepness of 20 waves is $a_0 k_0 = 0.01$ and vertical exaggeration 40:1.

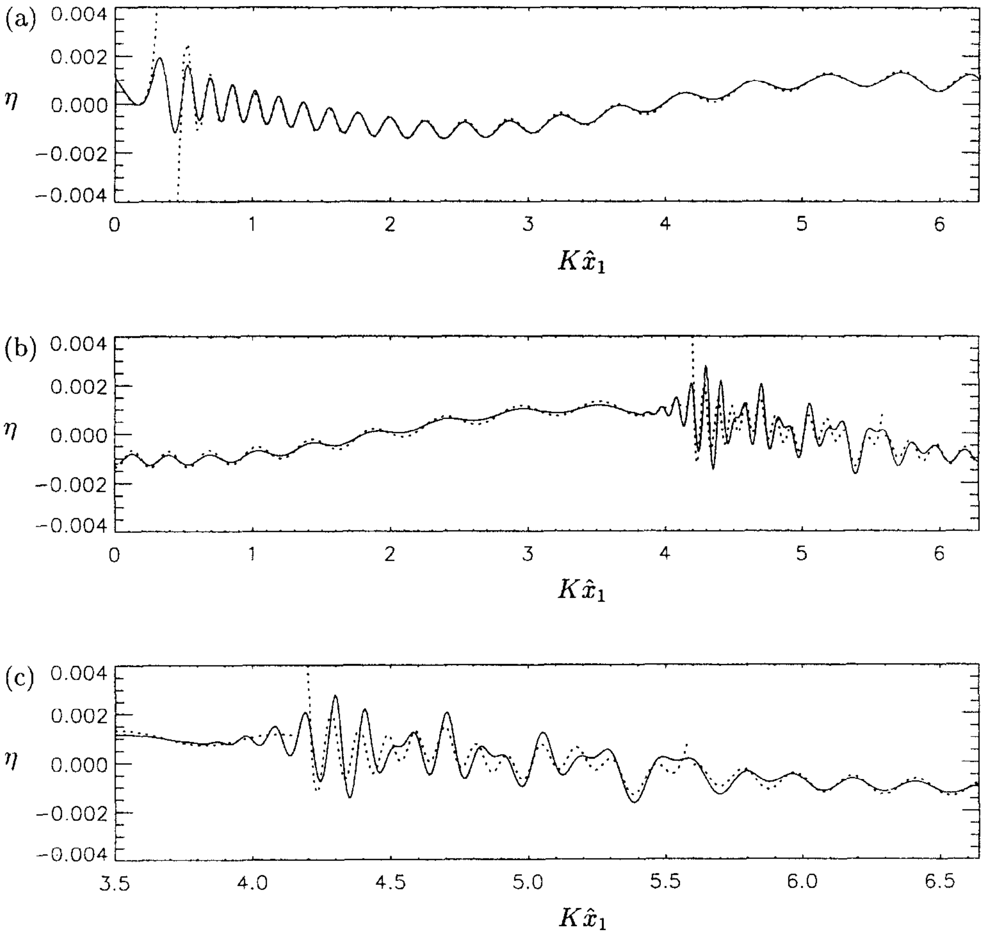

FIGURE 4. Comparing linear and nonlinear results: surface current = $U_c \cos(\hat{x} - 0.093t)$, $(\theta, \gamma) = (0.122, 2.416)$, fully nonlinear results (———), linear ray theory results (······), initial steepness of 20 waves is $a_0 k_0 = 0.01$, (a) $t = 60$, (b) $t = 106$ and (c) $t = 106$ showing more detail between the caustics.

5. Three-dimensional results

In three dimensions, we now consider an initial condition with a uniform wavetrain with wavenumber, $\underline{\boldsymbol{k}}$, at an angle α_0 say, to the current direction, thus introducing a fourth parameter into the problem. The coordinate system is shown in figure 5. From equation (4), we note that rays are only perpendicular to the crests in the absence of a current. Extension of the linear ray theory from one space to two space dimensions is numerically quite simple, especially since we have uniformity in the x_2-direction, and the only difficulty lies with the presentation of results, due to the large number of variables now present in the problem such as initial wavenumber, angle of propagation, position in (x_1, x_2, t) space etc. Results presented are for the same values of (θ, γ) as for the two dimensional case, except that now $\alpha_0 = \pi/6$.

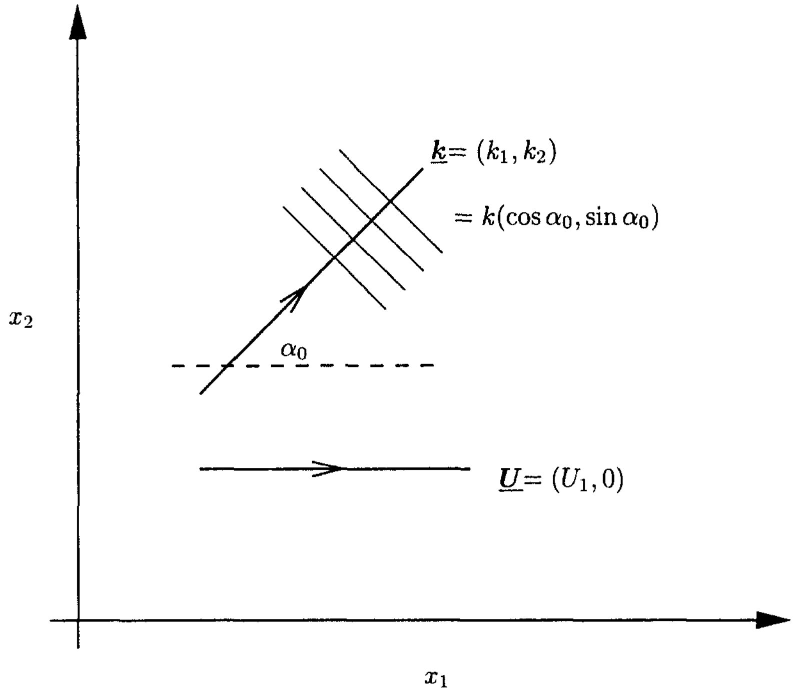

FIGURE 5. Initial wavetrain with crests an angle α_0 to the surface current direction.

As the current propagates only in the x_1-direction, the wavenumber, k_2 in the x_2-direction remains constant, as mentioned earlier. Without loss of generality we consider only the rays from $x_2 = 0$ since variation in the x_2-direction only arises from the different initial phases of the waves as x_2 varies. Figure 6 shows a ray diagram for $\alpha_0 = \pi/6$ and $(\theta, \gamma) = (0.122, 2.146)$ for the rays starting from $Kx_1 \in [0, 2\pi]$ and $x_2 = 0$. Note that this ray diagram is presented in a moving frame of reference as opposed to figure 2, which is presented in a fixed frame of reference. The rays have focussed in two regions indicated by C_I and C_{II}.

The focus in region C_I looks very similar to the type of focus we found in the two-dimensional case. We could think of the situation as qualitatively similar to having an initial wavenumber of k_1 in the x_1-direction, giving an effective γ to be $(g/k_1)^{\frac{1}{2}}/V \sim 2.60$ i.e. a larger value of γ which means we expect the focus to occur later (according to the work given in DPS). This is indeed the case here.

The second focus in region C_{II} is expected following the work of Peregrine and Smith [9] on steady wave fields. In figure 7 of their paper on nonlinear effects near caustics, they show part of the linear dispersion relation for waves on a uni-directional current $U(x)\underline{i}$. This figure shows that for a range of values of $k_2 g/\omega^2$, two caustics form, as opposed to the usual one in this steady situation. The two caustics are of different - 'R' and 'S' - types, and we expect this situation to be related to that here, where we get one or two foci depending on our value of α_0. This is a topic for further investigation.

The colour variation on figure 6 indicates the angle α between the direction of the propagating current, and the wavenumber $\underline{k}$. The basic behaviour of α can be explained in terms of the focussing and defocussing effect of the surface current generated by the internal wave. The wavenumber in the x_2-direction remains constant for all time. In the region $Kx_1 \in [0, \pi]$ the current has a focussing effect which also increases the wavenumber, k_1, in the x_1-direction, which in turn decreases the angle α i.e. the waves turn towards the direction of the propagating current. As the phase speed of the waves relative to the water decreases as the wavenumber increases, the waves in this region are slowed down. Conversely, in the region $Kx_1 \in [\pi, 2\pi]$, the surface current has a defocussing

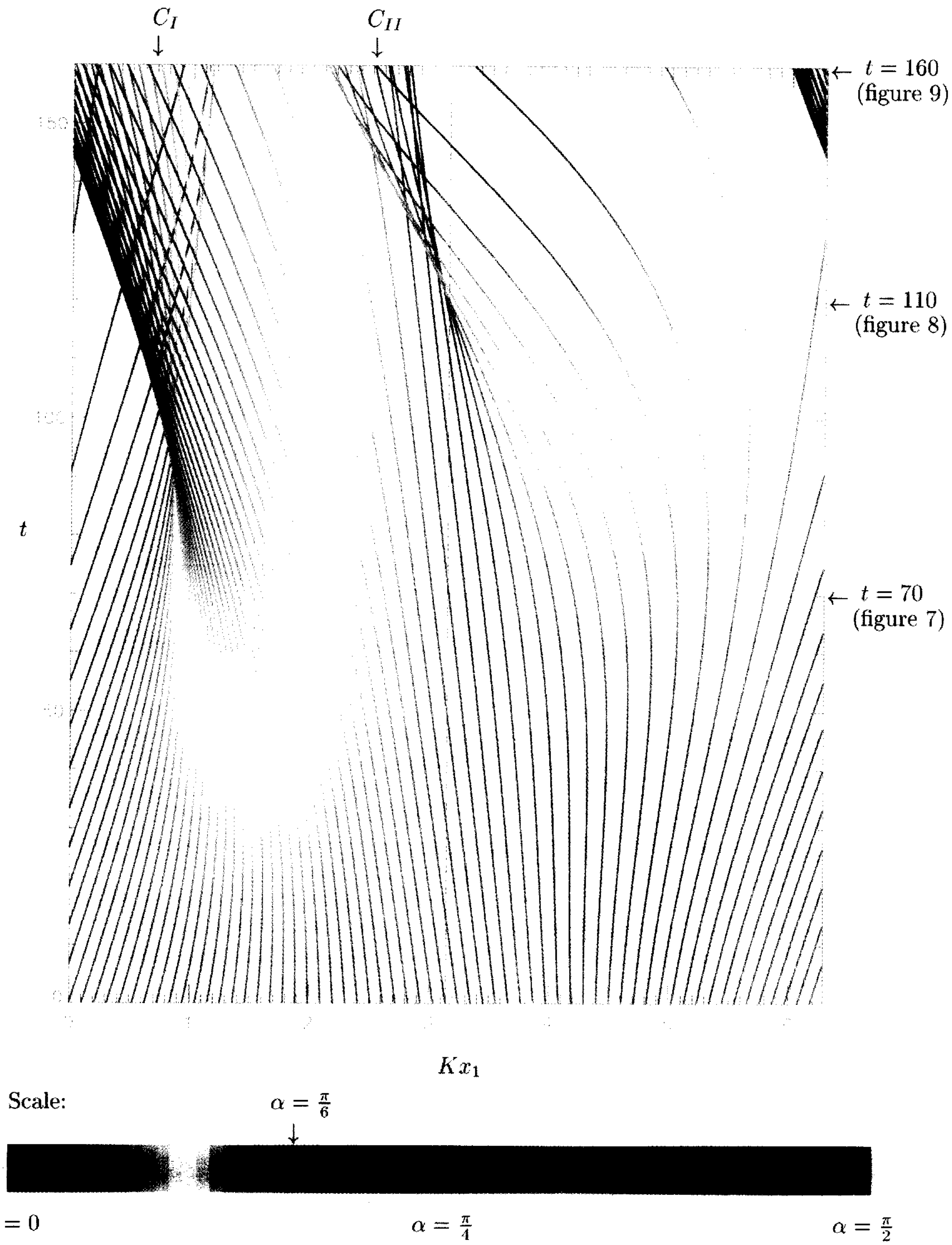

FIGURE 6. Ray diagram in the (x_1, t) plane showing the variation of angle α (with $(\theta, \gamma) = (0.122, 2.416)$ and $\alpha_0 = \pi/6$).

effect in the x_1-direction, k_1 decreases and the waves become longer. The value of α is increased and these long waves turn away from the direction of the propagation current.

Figures 7 to 9 show representations of the 'sea' surfaces corresponding to figure 6 for times: $t = 70$, $t = 110$ and $t = 160$ respectively in a frame of reference moving with the internal wave. These times are indicated on figure 6. The grey scale is chosen to show the waves with small steepnesses where we are confident about the predictions by linear ray theory. As ray theory predicts infinite values for amplitudes in regions where neighbouring rays cross, a cut off value for wave steepness is taken in figures 7 to 9 at $ak = 0.40$, as in our two-dimensional results. Regions where steepnesses exceed this value are shown in white. In practice, these are regions where nonlinear and/or diffractive effects are important. Black lines on figures 7 to 9 indicate the troughs of the waves. That is, in regions C_I and C_{II} indicated on figure 6, where there are three overlapping wave trains, there are three sets of lines.

Figure 7 shows the surface predicted by linear ray theory at $t = 70$, a time just prior to the first focus. The effect of the current on the wavenumber magnitude and direction of the surface waves is clearly seen. At $Kx_1 \sim 1$, the waves are being focussed. That is, they have become shorter and steeper - we note that steeper waves are indicated on these figures by a sharp black/white contrast. In addition, the direction of these focussing waves has changed from at $t = 0$ - they have moved so as to propagate more in the direction of the propagating current. Conversely away from this region where $Kx_1 \in [\pi, 2\pi]$, the waves have become longer and less steep. Also, as indicated by the colour variation on figure 6, the waves have turned away from the direction of the propagating current.

Figure 8 shows the surface at $t = 110$. This is a time shortly after the first focus and before the second focus. Region C_I indicated on on this figure is a region of three overlapping wavetrains. The easiest way to comprehend this wave formation is to once again refer to the ray diagram, figure 6. One wave train - 'on top' - enters region C_I from the right. These waves have the smallest value of α, i.e. they have turned to propagate almost in the direction with the current; they are the shortest waves. The second wave train enters 'below' from the left; this is made up of longer waves which have propagated from the region $Kx_1 \in [\pi, 2\pi]$, and are travelling with larger α values i.e. away from the current direction. The third wavetrain is generated from the 'fan' of rays which comes from the focus and adjacent caustics. These rays have less energy and have less effect on the form of the final surface pattern - they merely modulate the criss-cross pattern formed by the other two wave trains. The resultant pattern in region C_I is actually easier to see at a later time when the area covered is larger, as shown in figure 9. In a physical situation, one would expect to see a region of steep waves where a set of longer waves propagating at an angle to the direction of the current meets a set of shorter waves almost collimated with the current. At $Kx_1 \sim \pi$, a second focus made up of longer waves is forming. These long waves are steeper than the surrounding waves and they are propagating at a large angle to the direction of the current.

Figure 9 shows the surface at $t = 160$ after the second focus has formed. There are now two regions of three overlapping wavetrains. The form of the focus in region C_I is as discussed for figure 8, but the region is now much larger. Region C_{II} is formed of longer waves overlapping, so the crests of the resultant waves are of a different form. In this case, the wavetrain made up of the shorter waves enters from the left and the longer waves enter from the right. The crests in region C_I are short and thin, whereas the crests in region C_{II} are more circular. Note that this figure more clearly shows the phase jump of $\pm\pi/2$ at the caustics by the discontinuities in the black lines indicating the position of the wave troughs.

Figures 7 to 9 are an attempt to give snapshots of the surface at one time. The underlying wavetrains are of course moving. If two non-collinear wavetrains are superposed, the surface pattern is such that there is another moving frame of reference in which the surface is stationary. This is generally not the case for the superposition of waves in the focussing region formed of three wave trains here, in regions C_I and C_{II}, which are essentially unsteady wave patterns when viewed on the wave scale. However, the relative unsteadiness of these two regions is different. Region C_I is a fast modulation of the shorter waves (seen to the left of the focussing region) and will therefore be moving less quickly than region C_{II} which is, conversely, a slow modulation of the longer waves (again seen to the left).

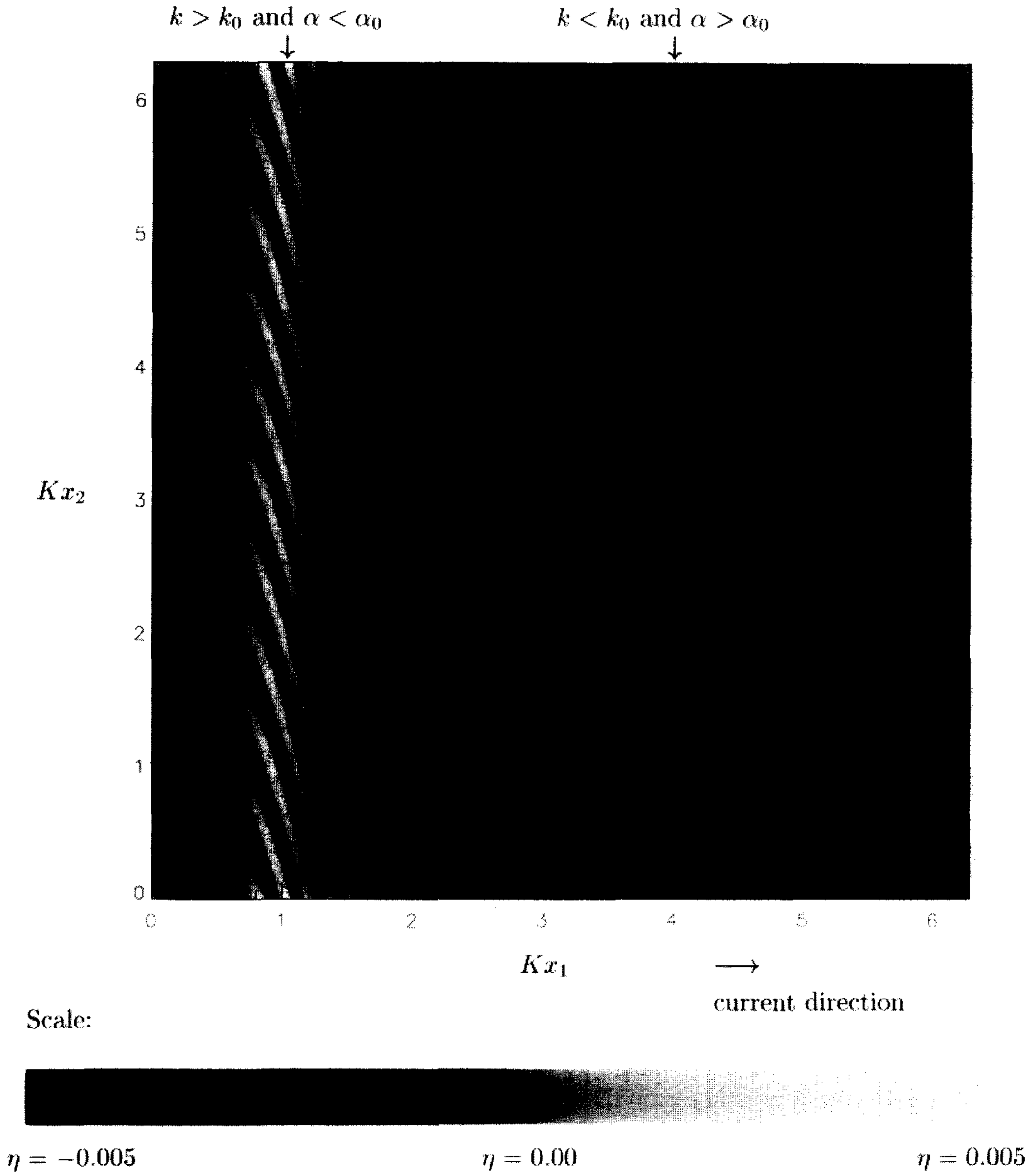

FIGURE 7. Wave surface at time $t = 70$ (with $(\theta, \gamma) = (0.122, 2.416)$, $\alpha_0 = \pi/6$ and $a_0 k_0 = 0.01$).

6. Conclusion

After utilising a fully nonlinear potential solver to justify the use of the linear ray theory in two dimensions, we have presented three-dimensional results showing wave-current interactions using this method. We have

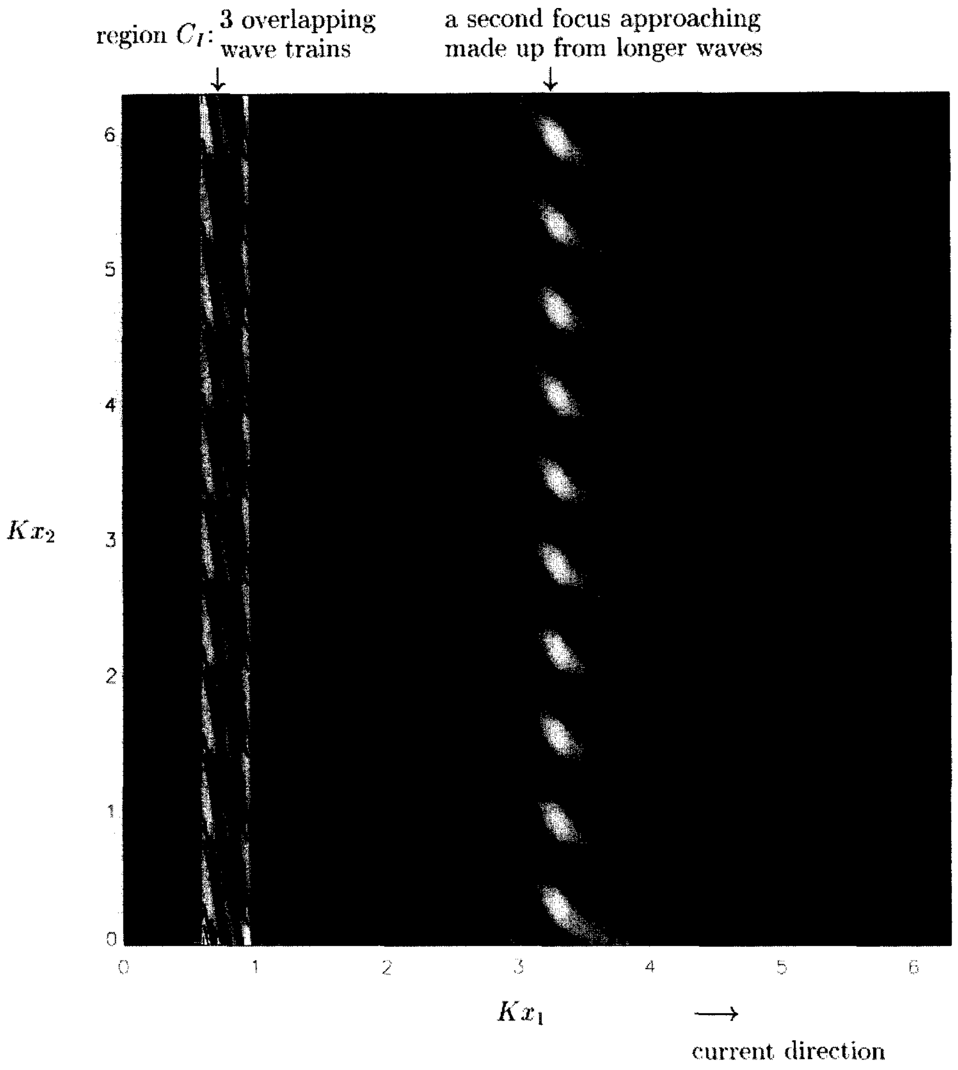

FIGURE 8. Wave surface at time $t = 110$ (with $(\theta, \gamma) = (0.122, 2.416)$, $\alpha_0 = \pi/6$ and $a_0k_0 = 0.01$).

restricted our presentation to one case, taking an initial angle of $\alpha_0 = \pi/6$ between the direction of the propagating current and a set of short surface waves of constant wavenumber; the strength of current and number of initially short waves we have chosen was a situation where, in the two dimensional case, the waves were strongly refracted and a focus formed. The main result we see is that in the region of converging streamlines of the surface current, two foci form. The first focus is of a similar form to that found in the two dimensional case consisting of very short waves, whereas the second is made up longer waves. The short waves are collimated by the current variation, and the longer waves propagate away from the direction of the current. The explanation

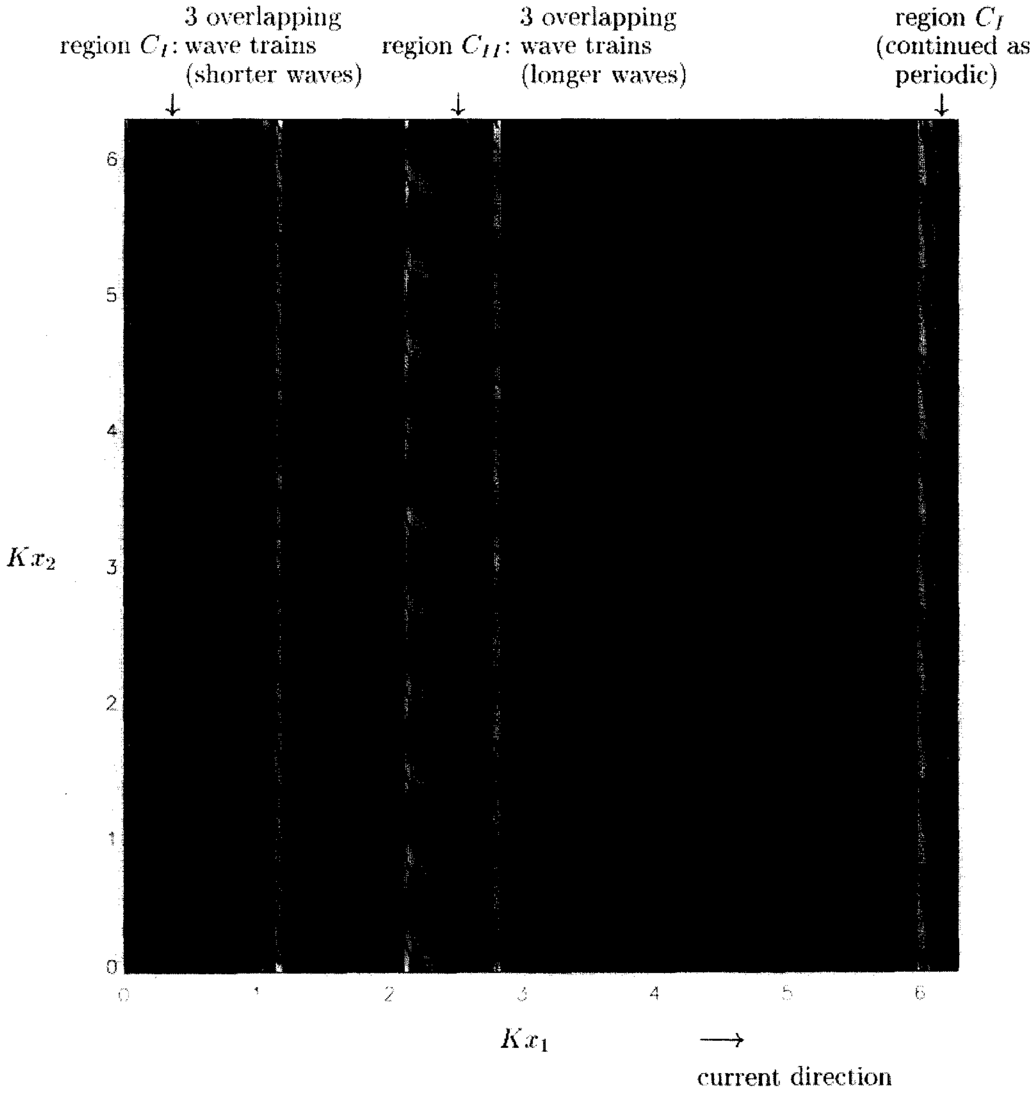

FIGURE 9. Wave surface at time $t = 160$ (with $(\theta, \gamma) = (0.122, 2.416)$, $\alpha_0 = \pi/6$ and $a_0 k_0 = 0.01$).

given for the wave behaviour in three dimensions is roughly explained in terms of the convergence and divergence of the surface current.

Consideration of a wider range of initial angles shows that there is a range of α_0 within $(0, \pi/2)$ which will give two foci for certain values of the velocity ratio parameters (θ, γ). The approach of Peregrine and Smith [9] on steady caustics in two dimensions should help to explain this phenomena, and this is the subject of further work which also includes the use of a current-modified nonlinear Schrödinger equation to model nonlinear effects in two and three dimensions pre-focussing.

Since the wave refraction depicted here occurs within a single wavelength of the underlying internal wave, it is unlikely that the type of wave patterns obtained depend strongly on the precise, sinusoidal current variation that is chosen. Indeed, focussing is a generic property of ray solutions, and hence we can expect focussed wave regions such as those shown here to arise on other unsteady current fields. Note the two different types, one representing a collimation of short waves towards the current direction and the other giving a strongly three-dimensional and unsteady surface pattern.

Acknowledgments

We would like to acknowledge the financial support of the D.E.R.A. and Alice Donato and Mark Jervis for their work on the fully nonlinear code.

References

[1] Peregrine, D.H. Interaction of water waves and currents. Adv. in Appl. Mech. 16 (1976) 9-117.
[2] Jonsson, J.J. Wave-current interactions. The Sea. Ocean Engineering Science 9, Part A (Eds. B. le Mihauti & D.M. Haine), Wiley-Interscience, 1990, pp.65-120.
[3] Gargett, A.E. & Hughes, B.A. On the interaction of surface and internal waves. J. Fluid Mech. 52 (1972) 179-191.
[4] Donato, A.N., Peregrine, D.H. & Stocker, J.R. The focussing of surface waves by internal waves, J. Fluid Mech. 384 (1999) 27-58.
[5] Dold, J.W. & Peregrine, D.H. An efficient boundary-integral method for steep unsteady water waves. Numer. Meth. for Fluid dynamics II (Eds. K.W.Morton & M.J.Baines), Oxford University Press, 1986, pp.671-679.
[6] Crapper, G.D. Introduction to water waves. Ellis Horwood Ltd, 1984.
[7] Rizk, M.H. & Ko, D.R.S. Interaction between small-scale surface waves and large-scale internal waves. Phys. Fluids 21 (1978) 1900-1907.
[8] Marston, P.L. Geometrical and catastrophe optics methods in scattering, in: High frequency pulse scattering (Eds. A.D. Pierce & R.N. Thurston), Physical Acoustics vol. XXI, Academic press, 1992 pp.1-234.
[9] Peregrine, D.H. & Smith, R. Nonlinear effects upon waves near caustics. Phil. Trans. A 292 (1979) 341-370.